Molecular Knots

DOI: 10.1002/anie.201302425

Simultaneous Self-Assembly of a [2]Catenane, a Trefoil Knot, and a Solomon Link from a Simple Pair of Ligands**

Thirumurugan Prakasam, Matteo Lusi, Mourad Elhabiri, Carlos Platas-Iglesias, John-Carl Olsen, Zouhair Asfari, Sarah Cianférani-Sanglier, François Debaene, Loïc J. Charbonnière, and Ali Trabolsi**

Beyond their aesthetic appeal, molecular links and knots are worthy synthetic targets that expand the chemist's repertoire of potential building blocks for engineering nanoscale devices.[1–8] [2]Catenanes ([2]Cs), trefoil knots (TKs), and Solomon links (SLs) are three such idealized topologies that have been realized synthetically.[9] Although a wide variety of [2]Cs (mechanically interlocked molecules comprised of two macrocycles) have been synthesized by statistical, covalent, or template-directed methods,[10–13] there are significantly fewer examples of efficient construction of molecular TKs and SLs,[1–2,9a] and examples of ligand systems that are able to provide two or more topological links in one pot are even more exceptional.[14]

The trefoil (or overhand) knot is a topologically nontrivial structure comprised of a single component that has three crossings and is unconditionally chiral.[1,15] The groundbreaking molecular synthesis was reported in 1989 by Sauvage and Dietrich-Buchecker,[16] and was followed by several other elegant syntheses.[9a;17]

The Solomon link is comprised of two closed loops with four crossings and can be regarded as a doubly braided [2]C. Examples of molecular SLs are rare,[18] and their preparation remains a challenge for chemists.

Metal templation is a well-established strategy for the formation of mechanically interlocked molecules and molecular knots. Recently, this approach has been augmented by the dynamic covalent chemistry (DCC) of imine ligands.[19] This hybrid strategy relies on reversible (metal–ligand and imine) bond formation, which allows in situ correction of structural errors and leads to increased yields of thermodynamically stable products in one reaction step.[1,8,19c] It can be

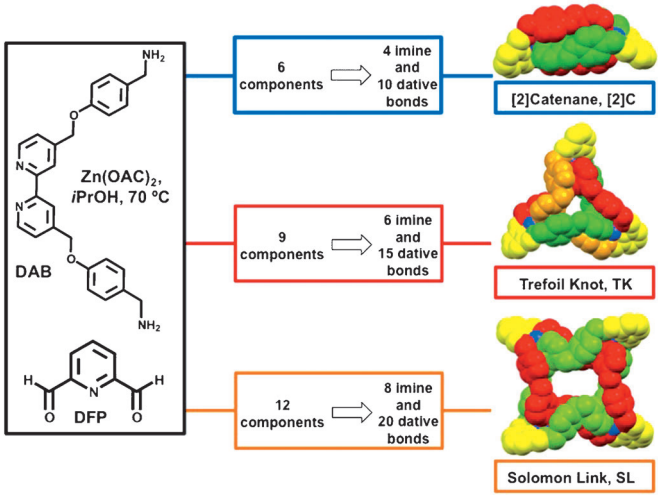

Scheme 1. One-pot synthesis of the [2]catenane ([2]C), the trefoil knot (TK), and the Solomon link (SL). All three structures were obtained from the starting materials (left) diaminobipyridine (DAB), diformylpyridine (DFP), and zinc acetate $Zn(OAc)_2$. The space-filling representations (right) are energy-minimized structures obtained with the aid of computational modeling (semiempirical PM6 calculations).

[*] Dr. T. Prakasam, Dr. M. Lusi, Prof. A. Trabolsi
Centre for Science and Engineering, New York University
Abu Dhabi (NYUAD) (United Aarab Emirates, UAE)
E-mail: ali.trabolsi@nyu.edu
Dr. M. Elhabiri
Laboratoire de Chimie Bioorganique et Médicinale, UMR 7509
CNRS-Université de Strasbourg, ECPM
25 rue Becquerel, 67087 Strasbourg (France)
Dr. C. Platas-Iglesias
Departamento de Química Fundamental, Universidade da Coruña
Campus da Zapateira
Rúa da Fraga 10, 15008 A Coruña (Spain)
Prof. J.-C. Olsen
School of Sciences, Indiana University Kokomo
Kokomo, IN 46904 (USA)
Dr. S. Cianférani-Sanglier, Dr. F. Debaene
Laboratoire de Spectrométrie de Masse Bio-Organique, IPHC, UMR 7178 CNRS-Université de Strasbourg, ECPM
25 rue Becquerel, 67087 Strasbourg (France)
Dr. Z. Asfari, Dr. L. J. Charbonnière
Laboratoire d'Ingénierie Moléculaire Appliquée à l'Analyse, IPHC
UMR 7178 CNRS-Université de Strasbourg, ECPM
25 rue Becquerel, 67087 Strasbourg (France)
E-mail: l.charbonn@unistra.fr

[**] The research described herein was sponsored by the New York University Abu Dhabi (NYUAD), in the UAE. T.P., M.L., and A.T. thank the NYUAD for generous support. M.E., S.C.S., F.D., Z.A., and L.C. thank the Centre National de la Recherche Scientifique (CNRS), the University of Strasbourg, and the Region Alsace in France for financial support. C.P.I. thanks Centro de Supercomputación de Galicia (CESGA) for providing the computer facilities. We thank A.C. Fahrenbach for useful discussions and B. Curzadd for the 3D cartoons.

Supporting information for this article is available on the WWW under http://dx.doi.org/10.1002/anie.201302425.

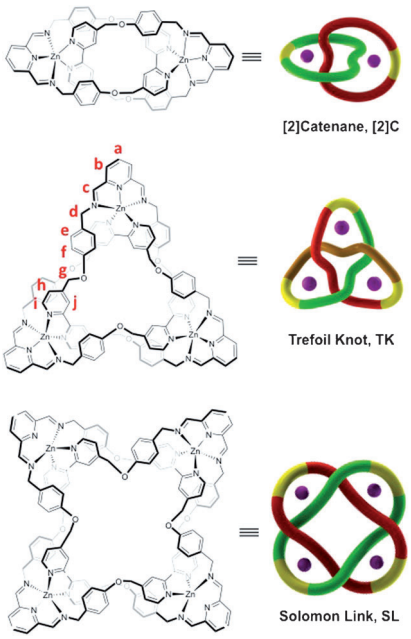

Figure 1. Chemical structures and graphical representations of [2]C, TK, and SL. Constitutionally heterotopic hydrogen atoms of TK are labelled from *a* to *j*.

distinguished from other methods that are carried out in one pot but involve multiple steps, or that require irreversible, kinetically controlled link-closing reactions such as alkylation.[1,8,18c,19c] In 2004, Stoddart and co-workers used the hybrid protocol to synthesize molecular Borromean rings (BRs), a link composed of three mechanically interlocked macrocycles.[20,21] Using the same ligand system, Solomon links were isolated instead of Borromean rings when a 1:1 mixture of Cu^{II} and Zn^{II} was added as template instead of only Zn^{II},[22] a result which emphasizes the large impact that subtle variations can have in such complex assembly processes.

Here we describe a simple pair of ligands, diformylpyridine (DFP) and diamino-2,2′-bipyridine (DAB), which, when combined with Zn^{II} ions, self-assemble into three complex structures (Scheme 1): a [2]catenane ([2]C), a trefoil knot (TK), and a Solomon link (SL), in a single pot. This system showcases the combined power of metal templation and DCC of imine ligands to generate concomitantly the three links.

In the case of the BRs,[20] strong intramolecular π–π stacking interactions between bipyridyl and phenoxy moieties of adjacent ligand strands were shown to be crucial to the structural integrity of the complex. We anticipated that symmetrical insertion of methylene groups between the bipyridyl and phenoxy units of the diaminopyridine ligand of the BRs would maintain the structurally important π–π stacking interactions, but would also provide enough rotational freedom and flexibility for the ligand strands to self-assemble into a variety of alternative and topologically nontrivial structures, such as 2[C], TK, or SL. Molecular modeling (PM6 calculations, see the Supporting Information) of these three structures was consistent with our expectations.

The DAB ligand was synthesized in eight steps from commercially available starting materials (see the Supporting Information for complete experimental details). Mixing stoichiometric amounts of DFP, $Zn(OAc)_2$, and the hydrotrifluoroacetate salt of DAB in isopropanol (*i*PrOH) at 70 °C for four hours led to the formation of a precipitate which was collected by filtration and washed with *i*PrOH and dichloromethane to give the TK as a yellowish solid in 56% yield. High-resolution electrospray-ionization mass spectrometry (HRMS) of the compound dissolved in MeOH showed three major peaks (Figure S14A in the Supporting Information) with maxima at *m*/*z* 1111.692, 704.134, and 499.355, which correspond to $[TK{\cdot}4\,TFA]^{2+}$, $[TK{\cdot}3\,TFA]^{3+}$, and $[TK{\cdot}2\,TFA]^{4+}$, respectively (TFA = trifluoroacetate). The isotopic distributions of these peaks are in full agreement with their calculated patterns.

After the TK precipitate was separated from the reaction mixture, slow evaporation of *i*PrOH produced tiny cubic crystals. HRMS analysis of the crystals (Figure S14B in the Supporting Informaton) showed two major peaks with maxima at *m*/*z* 704.132 and 431.760, which were consistent with $[[2]C{\cdot}2\,TFA]^{2+}$ and $[[2]C{\cdot}TFA]^{3+}$, respectively. The crystals were isolated in 22% yield. The mechanically interlocked structure (Figure 1) was further confirmed by ^1H NMR spectroscopy and X-ray crystallography (see Figures 2 and 3 and text below).

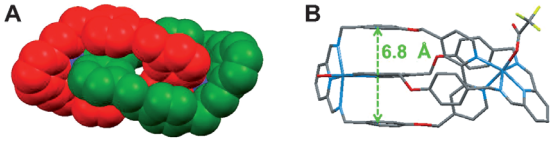

Figure 2. X-ray crystal structure of [2]C. A) Space-filling representation of the solid-state structure obtained from single-crystal X-ray analysis of [2]C. B) Side view of the wire-frame X-ray structure showing the π-(phenoxy···bipyridyl···phenoxy) triplet stacking between the two phenoxy rings of one macrocycle and the bipyridine unit of the other macrocycle.

[2]C crystallized in the triclinic $P\bar{1}$ space group with one [2]C molecule per asymmetric unit cell (Figure 2). Each molecule of [2]C is composed of two identical interlocked macrocycles held together by two Zn^{II} ions. Each macrocycle is the result of the condensation of one DAB and one DFP through the formation of two imine bonds. The Zn^{II} ions adopt a distorted octahedral geometry and are coordinated by the bidentate bipyridyl unit of one macrocycle and the tridentate diimino pyridyl moiety of the other macrocycle. A pair of phenoxy rings in each macrocycle sandwiches a bipyridyl moiety of the other macrocycle to form two compact π-(phenoxy···bipyridine···phenoxy) triplet stacks per [2]C. The phenoxy bipyridine distances (Figure 2B) are 3.4 Å. The sixth coordination site of one Zn^{II} ion is occupied by an oxygen atom of a TFA anion, while the other Zn^{II} ion is coordinated by an oxygen atom of a water molecule. The coordinated water molecule is hydrogen-bonded to two TFA anions.

The structures of [2]C and TK were also investigated in solution by ^1H NMR spectroscopy. ^1H NMR spectra (Figure 3) of [2]C, TK, and the free ligands DAB and DFP were measured in CD_3OD at room temperature. The

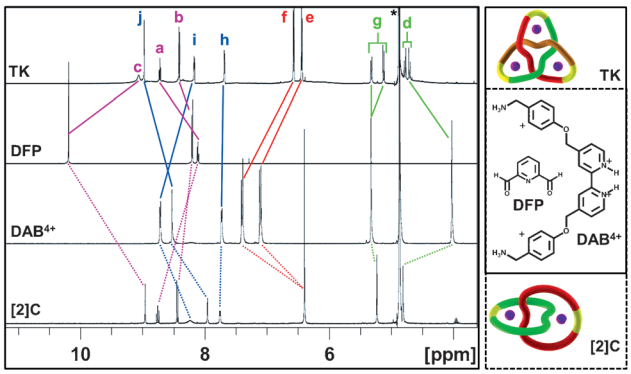

Figure 3. ^{1}H NMR spectra of TK and [2]C (600 MHz, CD_3OD, 298 K) aligned with those of the starting materials DAB (as its tetrahydrotrifluoroacetate salt DAB-H_4·4TFA) and DFP.

^{1}H NMR signals for the phenoxy hydrogen atoms *e* and *f* in the spectrum of [2]C are shifted upfield ($\Delta\delta = +0.78$ and $+1.07$ ppm, respectively) relative to their positions in the spectrum of DAB. The spectrum of TK is consistent with the presence of a single, highly symmetrical species in solution, with the *e* and *f* resonances also being upfield shifted ($\Delta\delta = +0.76$ and $+0.91$ ppm, respectively). For both [2]C and TK, these shifts are a strong indication of the increased shielding that the hydrogen atoms experience within the π–π stacking arrangements of the two structures. The downfield shifts of the *a* and *b* signals are similar for both topologies and are a consequence of Zn^{II} coordination. Regarding the signals of the bipyridyl protons, while *h* remains nearly unchanged in the spectra of [2]C, TK, and DAB, *i* is shifted upfield in [2]C and TK as a consequence of Zn^{II} complexation and the concomitant *syn* conformation of the bipyridyl moieties. Importantly, the *j* signal allows for distinctions to be made between the two structures in relation to the sizes of their cavities. With respect to its position in the spectrum of DAB, the *j* proton resonance is shifted upfield by $+0.75$ ppm in the spectrum of [2]C and downfield by -0.51 ppm in the spectrum of TK. Close examination of the crystal structure of 2[C] and the PM6 model of TK shows that the *j* protons of 2[C] are in close proximity to the *j* protons of the second macrocyle (2.54 Å), whereas the corresponding distance in TK (3.67 Å, Figure S12 in the Supporting Information) is far longer. Different degrees of solvent exposure might also be responsible, in part, for the observed chemical shift differences. Another significant difference between the spectra of the two links involves the methylene resonances *g* and *d*. For both [2]C and TK, the *g* signal is shifted upfield and the *d* signal is shifted downfield relative to their respective positions in the spectrum of DAB. However, whereas the *g* and *d* signals are singlets in the spectrum of [2]C (as a result of an effective C_{2v} symmetry), they are each split into doublets in the spectrum of TK, reflecting the diastereotopic nature of these protons brought about by the knot topology. A ^{1}H NMR spectrum recorded in the presence of Pirkle's reagent (Figure S11 in the Supporting Information) further confirms the chirality of TK. Numerous multiplets in this spectrum indicate the formation of diastereomeric complexes composed of the enantiomers of TK and the optically pure reagent. Diffusion-ordered NMR spectroscopy (DOSY) showed diffusion coefficients for [2]C and TK of 5.38×10^{-10} $m^2 s^{-1}$ and 4.31×10^{-10} $m^2 s^{-1}$, respectively, and further distinguished the two links (Figure S9 in the Supporting Information).

The evolution of intermediate formation was monitored by HRMS. After the temperature of the reaction had reached 70 °C ($t = 0$ min), aliquots of the reaction mixture were removed after $t = 0$, 15, 30, 45, 60, 120, 180, 300, and 3600 min, and the solid and solution phases of each aliquot were separated by centrifugation and analyzed by HRMS in H_2O:MeCN (1:1 by volume; see the Supporting Information for experimental details). Characteristic peaks for $[[2]C{\cdot}TFA]^{3+}$ (max. at $m/z = 431.760$) and $[TK{\cdot}TFA]^{5+}$ (max. at $m/z = 376.887$) were present in the mass spectrum of the very first aliquot of the solution phase ($t = 0$). Peaks corresponding to SL were first detected in the aliquot that was removed after 30 minutes and in all subsequent aliquots. Separate analysis of the precipitates showed a gradual disappearance of DAB and increasing amounts of both SL and TK. In the solid samples, over the course of one hour, the relative intensities of SL and TK peaks changed markedly, with those corresponding to the SL gradually decreasing to very low levels, and those corresponding to TK remaining prominent.

A thorough analysis of the first 30 minutes of the reaction was particularly informative regarding the presence of several key-intermediate species (Figure S22 in the Supporting Information). Peaks corresponding to the general formula $[Zn_xDAB_yDFP_z\text{-}nH_2O]$ (hereafter abbreviated as *xyz*-nH_2O) could be arranged in an order that suggests a mechanistic pathway leading to all three products as depicted in Figure 4 (details of the MS results are reported in Figure S22 in the Supporting Information).

The presence of 2[C] and TK in the first minutes of the reaction together with the transient appearance of SL followed by its disassembly clearly indicates that the assembly/disassembly processes occur on the time scale of minutes in solution.

At no point during the reaction were oligomers of DAB and DFP detected in the dynamic library. The only species discovered were [2]C, TK, SL, and their associated intermediates. These observations are consistent with a key feature of the assembly process: apart from the very first condensation between DFP and DAB to form the 011-H_2O intermediate (Figure 4), the addition of DFP is always accompanied by the addition of a Zn^{II} cation and the loss of water through imine bond formation. This suggests that elongation results from the coordination of a Zn(DFP) to a bipyridyl moiety, with imine bond formation catalyzed by Zn^{II} and π–π stacking interactions. It is the acute curvature of each newly added Zn(DFP) chelate and the clamping of the chelate to a bipyridyl unit by π–π stacking that ensure that a growing structure forms a discrete link in a limited number of steps rather than an extended linear oligomer of variable length. Others have described the phenomenon of template-directed macrocylization[23] and how noncovalent forces facilitate the synthesis of large rings and avoid the formation of linear oligomeric side products. In our experiments, neither linear species nor free macrocycles were observed. This result

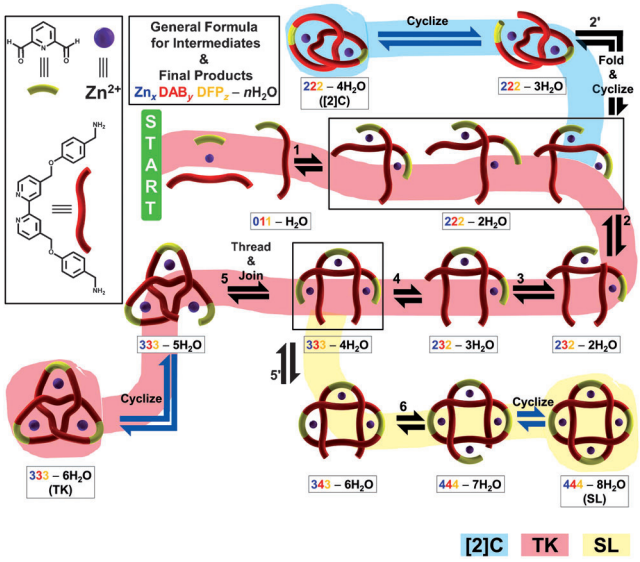

Figure 4. Mechanistic pathway for the formation of [2]C, TK, and SL. The color-coded pathway illustrates a possible mechanistic route that was inferred from species detected by HRMS analysis. Species are designated by the abbreviated formulas *xyz*-*n*H_2O, where *x*, *y*, and *z* correspond to the subscripts for Zn^{II}, DAB, and DFP, respectively, and *n* is the number of water molecules lost through imine bond formation.

highlights the strong, template-directed propensity of our system to form links.

Of the three links that were formed, [2]C and TK were favored. SL was observed in both solid and liquid phases during the reaction; however, its presence was transient. The reversible nature of imine bond formation allowed for its conversion to smaller structures. This impermanence suggests that SL is thermodynamically less stable than either [2]C or TK and is consistent with computational modeling experiments. For example, the angles between the averaged planes of the bipyridyl units and the phenoxy rings were found to be 11.7° in SL versus 7.4° in both TK and [2]C, a difference of 4.3° that points to weaker π–π stacking in SL.

The relative thermodynamic stabilities of [2]C and TK were more difficult to determine. However, ^{1}H NMR, X-ray, and computational data seem to indicate that [2]C is the most stable molecule. Strong evidence indicates that [2]C is more compact than TK. The H*j*–H*j* distance in [2]C was found by X-ray analysis to be only 2.54 Å (Figure S13 in the Supporting Information), whereas in TK, this distance was determined by computational modeling to be 3.67 Å (Figure S12 in the Supporting Information). The shorter distance in [2]C is corroborated by the larger upfield shift of its *j* proton resonances in the ^{1}H NMR spectra. Furthermore, the calculated volumes of the two structures are 1318 and 2206 Å^3 for [2]C and TK, respectively, corresponding to 659 and 735 Å^3 per Zn(DAB)(DFP) subunit. The greater compactness of [2]C suggests stronger intramolecular attractions, which are enthalpically favorable. The angles between the bipyridyl and phenoxy rings in both molecules were determined by computational modeling to be 7.4°, in other words, small and conducive to π–π stacking interactions. (In the case of [2]C, the calculated structure and X-ray analysis are in excellent agreement). Nevertheless, [2]C has a specific enthalpic advantage over TK as the result of having nearly distortion-free bipyridyl dihedral angles. In [2]C, both of these angles are 8.8°, whereas in TK, they are 2.8, 6.9, and 15.4°, the latter being a significant and energetically unfavorable deviation, one that may contribute to the more positive heat of formation calculated for TK (−37.70 kcal mol^{-1}) versus [2]C (−48.99 kcal mol^{-1}). Finally, the physical behavior of the reaction itself supports the conclusion that [2]C is more stable. Although the equilibrium is shifted by the precipitation of TK, [2]C remains the major product in solution, even after 4 hours of reaction. Assuming a higher stability for TK, one would expect a complete displacement of the reaction equilibrium toward TK, but such a displacement does not occur.

In summary, we have utilized a simple pair of chelating ligands that, when combined with Zn^{II} ions, furnishes three topologically nontrivial structures: a [2]catenane, a trefoil knot, and a Solomon link in an all-in-one-pot reaction. The [2]catenane, [2]C, was isolated from the solution phase of the reaction, whereas the trefoil knot, TK, precipitated and was isolated by filtration. The Solomon link, SL, was only detected by mass spectrometry. The formation of all three products can be rationalized by a mechanism deduced from mass spectrometry data. Mass spectrometric kinetic analysis of the reaction suggests that [2]C and TK are thermodynamically more stable than the SL, which appears only transiently. The pair of ligands, DFP and DAB, are achiral and produce the achiral [2]C, as well as racemic mixtures of TK and SL, which are both topologically chiral. The adjustment of metal–ligand, dynamic covalent, and π–π stacking interactions in modular systems of this type provides access to a range of target molecules from simple precursors. Our results and those of others[17h–i,19] demonstrate that the all-in-one metal-templation/DCC synthetic strategy is a powerful method for the design and synthesis of molecular knots and links.

Received: March 22, 2013
Revised: May 2, 2013
Published online: July 5, 2013

Keywords: catenanes · dynamic covalent chemistry · metal templation · Solomon link · trefoil knot

[1] R. S. Forgan, J.-P. Sauvage, J. F. Stoddart, *Chem. Rev.* **2011**, *111*, 5434 – 5464.
[2] "Templates in Chemistry II": C. Dietrich-Buchecker, B. Colasson, J.-P. Sauvage, *Topics in Current Chemistry*, *Vol. 249*, Springer, Berlin, **2005**, pp. 261 – 283.
[3] J.-F. Ayme, J. E. Beves, C. J. Campbell, D. A. Leigh, *Chem. Soc. Rev.* **2013**, *42*, 1700 – 1712.
[4] E. E. Fenlon, *Eur. J. Org. Chem.* **2008**, 5023 – 5035.
[5] O. Lukin, F. Vögtle, *Angew. Chem.* **2005**, *117*, 1480 – 1501; *Angew. Chem. Int. Ed.* **2005**, *44*, 1456 – 1477.
[6] J.-M. Lehn, *Chem. Soc. Rev.* **2007**, *36*, 151 – 160.
[7] C. Dietrich-Buchecker, G. Rapenne, J.-P. Sauvage, *Molecular Catenanes, Rotaxanes and Knots*, Wiley-VCH, Weinheim, **2007**, pp. 107 – 142.
[8] J. F. Stoddart, *Chem. Soc. Rev.* **2009**, *38*, 1802 – 1820.

[9] a) N. Ponnuswamy, F. B. L. Cougnon, J. M. Clough, G. D. Pantoş, J. K. M. Sanders, *Science* **2012**, *338*, 783 – 785; b) F. Davis, S. Higson, *Macrocycles: Construction, Chemistry and Nanotechnology Applications*, Wiley, Chichester, **2011**, pp. 381 – 517.
[10] J. D. Crowley, S. M. Goldup, A.-L. Lee, D. A. Leigh, R. T. McBurney, *Chem. Soc. Rev.* **2009**, *38*, 1530 – 1541.
[11] C. O. Dietrich-Buchecker, J.-P. Sauvage, J. M. Kern, *J. Am. Chem. Soc.* **1984**, *106*, 3043 – 3045.
[12] S. Durot, F. Reviriego, J.-P. Sauvage, *Dalton Trans.* **2010**, *39*, 10557 – 10570.
[13] F. M. Raymo, J. F. Stoddart, *Molecular Catenanes, Rotaxanes and Knots*, Wiley-VCH, Weinheim, **2007**, pp. 143 – 176.
[14] a) H. Y. Au-Yeung, F. B. L. Cougnon, S. Otto, D. Pantos, J. K. M. Sanders, *Chem. Sci.* **2010**, *1*, 567 – 574; b) F. B. L. Cougnon, J. K. M. Sanders, *Acc. Chem. Res.* **2012**, *45*, 2211 – 2221.
[15] a) L. F. Liu, L. Perkocha, R. Calendar, J. C. Wang, *Proc. Natl. Acad. Sci. USA* **1981**, *78*, 5498 – 5502; b) L. F. Liu, R. E. Depew, J. C. Wang, *J. Mol. Biol.* **1976**, *106*, 439 – 452; c) S. Kamitori, *J. Am. Chem. Soc.* **1996**, *118*, 8945 – 8946; d) C. Liang, K. Mislow, *J. Am. Chem. Soc.* **1994**, *116*, 11189 – 11190; e) W. R. Taylor, *Nature* **2000**, *406*, 916 – 919.
[16] C. O. Dietrich-Buchecker, J.-P. Sauvage, *Angew. Chem.* **1989**, *101*, 192 – 194; *Angew. Chem. Int. Ed. Engl.* **1989**, *28*, 189 – 192.
[17] a) L.-E. Perret-Aebi, A. von Zelewsky, C. Dietrich-Buchecker, J.-P. Sauvage, *Angew. Chem.* **2004**, *116*, 4582 – 4585; *Angew. Chem. Int. Ed.* **2004**, *43*, 4482 – 4485; b) P. R. Ashton, O. A. Matthews, S. Menzer, F. M. Raymo, N. Spencer, J. F. Stoddart, D. J. Williams, *Liebigs Ann.* **1997**, 2485 – 2494; c) P. E. Barran, H. L. Cole, S. M. Goldup, D. A. Leigh, P. R. McGonigal, M. D. Symes, J. Wu, M. Zengerle, *Angew. Chem.* **2011**, *123*, 12488 – 12492; *Angew. Chem. Int. Ed.* **2011**, *50*, 12280 – 12284; d) C. O. Dietrich-Buchecker, J. Guilhem, C. Pascard, J.-P. Sauvage, *Angew. Chem.* **1990**, *102*, 1202 – 1204; *Angew. Chem. Int. Ed. Engl.* **1990**, *29*, 1154 – 1156; e) C. O. Dietrich-Buchecker, J.-P. Sauvage, A. De Cian, J. Fischer, *J. Chem. Soc. Chem. Commun.* **1994**, 2231 – 2232; f) C. O. Ditrich-Buchecker, J. F. Nierengarten, J. P. Sauvage, *Tetrahedron Lett.* **1992**, *33*, 3625 – 3628.
[18] a) J. F. Nierengarten, C. O. Dietrich-Buchecker, J. P. Sauvage, *J. Am. Chem. Soc.* **1994**, *116*, 375 – 376; b) C. P. McArdle, J. J. Vittal, R. J. Puddephatt, *Angew. Chem.* **2000**, *112*, 3977 – 3980; *Angew. Chem. Int. Ed.* **2000**, *39*, 3819 – 3822; c) C. D. Pentecost, K. S. Chichak, A. J. Peters, G. W. V. Cave, S. J. Cantrill, J. F. Stoddart, *Angew. Chem.* **2007**, *119*, 222 – 226; *Angew. Chem. Int. Ed.* **2007**, *46*, 218 – 222; d) C. Peinador, V. C. Blanco, J. M. Quintela, *J. Am. Chem. Soc.* **2009**, *131*, 920 – 921; e) C. P. McArdle, M. C. Jennings, J. J. Vittal, R. J. Puddephatt, *Chem. Eur. J.* **2001**, *7*, 3572 – 3583.
[19] a) D. A. Leigh, P. J. Lusby, S. J. Teat, A. J. Wilson, J. K. Y. Wong, *Angew. Chem.* **2001**, *113*, 1586 – 1591; *Angew. Chem. Int. Ed.* **2001**, *40*, 1538 – 1543; b) L. Hogg, D. A. Leigh, P. J. Lusby, A. Morelli, S. Parsons, J. K. Y. Wong, *Angew. Chem.* **2004**, *116*, 1238 – 1241; *Angew. Chem. Int. Ed.* **2004**, *43*, 1218 – 1221; c) M. E. Belowich, J. F. Stoddart, *Chem. Soc. Rev.* **2012**, *41*, 2003 – 2024.
[20] K. S. Chichak, S. J. Cantrill, A. R. Pease, S.-H. Chiu, G. W. V. Cave, J. L. Atwood, J. F. Stoddart, *Science* **2004**, *304*, 1308 – 1312.
[21] C. D. Meyer, R. S. Forgan, K. S. Chichak, A. J. Peters, N. Tangchaivang, G. W. V. Cave, S. I. Khan, S. J. Cantrill, J. F. Stoddart, *Chem. Eur. J.* **2010**, *16*, 12570 – 12581.
[22] a) S. J. Cantrill, K. S. Chichak, A. J. Peters, J. F. Stoddart, *Acc. Chem. Res.* **2005**, *38*, 1 – 9; b) K. S. Chichak, A. J. Peters, S. J. Cantrill, J. F. Stoddart, *J. Org. Chem.* **2005**, *70*, 7956 – 7962; c) K. S. Chichak, S. J. Cantrill, J. F. Stoddart, *Chem. Commun.* **2005**, 3391 – 3393.
[23] a) J.-M. Lehn, *Science* **2002**, *295*, 2400 – 2403; b) D. H. Busch, *Coord. Chem. Rev.* **1990**, *100*, 119 – 154; c) D. A. Leigh, A. Venturini, A. J. Wilson, J. K. Y. Wong, F. Zerbetto, *Chem. Eur. J.* **2004**, *10*, 4960 – 4969.

